Texas A&M Research Foundation

College Station, Texas

IMPROVEMENT OF PROPELLER STATIC THRUST ESTIMATION

NASA Research Grant No. NsG-669

Final Report For the Period

July 1, 1964 to August 31, 1965

Revised

Prepared by

A. E. Cronk
Research Engineer

Joseph C. Brusse
Assistant Research Engineer

Texas Engineering Experiment Station

January 1966

ABSTRACT 20085

This report describes the development of experimental facilities for the measurement of thrust and torque of model propellers operating in the static thrust condition. Techniques for flow visualization upstream and downstream of the plane of rotation of the propeller are described. A theoretical method for calculation of the inflow velocity field and propeller wake contraction is summarized. A computer program for numerical calculations following this theory is described.

INTRODUCTION

The work reported in this document has been accomplished under NASA Grant NsG 669. The Grant support started July 1, 1964, and was to continue for approximately one year. A request for a two month extension in time with no additional expense to the government was approved and resulted in a revised completion date for the grant of August 31, 1965.

The problem to be studied with the aid of funds provided by the NASA Research Grant is that of improving the performance estimation of propellers operating in the heavily loaded static thrust condition. The design of aircraft propellers by analytical methods which use the classical propeller theory ascribed to Goldstein has not been completely successful, particularly when performance optimization for the static thrust condition is attempted. The origin of the deficiencies in the analytical method is not apparent and consequently has caused considerable concern in the present development of propeller driven V/STOL Aircraft. In reality, propeller designers do not know whether the discrepancy between calculated and actual performance is to be attributed to propeller performance alone or to the effects of the vehicle to which the propeller is mounted. It is probable that both the propeller and the installation effects are responsible but the contribution of each to the overall performance can not be accurately estimated at this time.

In order to assess the Goldstein Theory as it applies to propellers operating in the static thrust condition, it was considered necessary to inaugurate an experimental investigation to evaluate the performance of propellers alone and then to attempt correlation of analytically developed performance data with the experimentally gene-

rated data. It is also considered necessary to acquire a more complete understanding of the actual airflow phenomena in the vicinity of the propeller in order that the basic assumptions involved in the existing analytical methods can be assessed. Critical evaluation of the several propeller performance analytical methods indicates that a better knowledge of the radial loading distribution as well as the inflow of air into the propeller is required. Consequently it appears necessary that the experimental apparatus permit measurement of the air-flow at the propeller plane of rotation and perhaps the actual measurement of the radial load distribution on the blade itself. It is felt that if the flow patterns in the real fluid are understood more completely, the development of an analytical method will be much more easily attained. The ultimate aim of the research supported by the NASA Grant is the development of an analytical method which will yield performance estimates that more nearly compare to the actual performance observed.

Although the original proposal required a critical evaluation of some of the Wright Field Whirl Test data, planning conferences subsequent to receipt of the Grant resulted in changing and realigning the objectives of the project. It was felt at that time that little value would accrue from a reevaluation of Wright Field Test Data and that since an improved static thrust estimation procedure was needed, work should commence at once in this direction.

The revised program called for the construction of a propeller static thrust dynamometer which would be adequate for conducting propeller performance experiments as well as the airflow studies mentioned in the preceding paragraph. In addition to the static thrust dynamometer, a program of study and development of analytical methods useful

in the prediction of propeller performance was to be carried out.

STATIC THRUST DYNAMOMETER

A propeller static thrust dynamometer designed to minimize wake and inflow interference has been constructed in a large airplane hangar at the Texas A&M Research Annex. The size and configuration of the dynamometer was determined after careful consideration of the following desirable features:

1. Test propellers must be isolated to the greatest degree possible.
2. The dynamometer must be capable of operating model propellers large enough to permit evaluation of Reynolds Number effects.
3. The facility should be installed inside a building to avoid the vagaries of the weather.

With these factors in mind a configuration was conceived wherein the propeller is mounted so that it rotates in a horizontal plane with the line of thrust acting vertically upward. The propeller is rotated by a vertical shaft which turns inside a 7.5 inch diameter tubular steel housing. The housing has four slanted legs welded to its lower end which are bolted to specially constructed reinforced concrete piers eleven feet deep in the earth. The propeller plane of rotation is 20 feet above the floor of the hangar and 10 feet below the roof joists. The curved hangar roof provides about 15 feet of additional overhead space that contains the roof supporting trusses. The nearest walls are in excess of 40 feet from the propeller. While the desirable condition of testing in an infinitely large air space has not been totally realized, it is believed the installation approximates this condition within

practical limits.

Preliminary calculations indicated that approximately 400 horsepower would be required to operate 5-foot diameter, 4-way, high activity factor propellers at tip speeds of 900 feet per second. In addition to providing these values of power and speed, the power source must be easily controllable through a wide speed range. In the interest of economy, internal combustion engines were chosen for the power source instead of an electric motor drive. Two 275-HP Chris Craft V-8 Marine engines are installed to drive the vertical shaft through a differential gear box. Couplings are installed at each engine output shaft to allow for installation misalignment and vibration isolation. An overrunning clutch is mounted between the differential gear box output shaft and the main drive shaft to provide protection for the propeller balance in the event of mechanical failure in either of the power trains or the gear box. A splined axial-slip coupling is provided between the upper end of the main drive shaft and NASA provided propeller shaft to allow for thermal expansion and contraction of the shafts. A NASA strain gaged propeller balance is mounted upstream of the thrust bearing and a propeller hub adapter shaft and propeller are then mounted directly to the balance. The electric signals from the balance are routed through a slip ring assembly and thence through conduit to amplifiers and the read-out gages. A 60-tooth steel gear is mounted on the propeller shaft between the balance and the thrust bearing to provide impulses through a magnetic pickup to an electronic tachometer. A small control house was built to house the power controls and the data acquisition equipment. The house has a large safety glass window through which the operator and an observer can view the propeller

dynamometer. Flexible electrical cables between the test rig and the control house are 40 feet long and allow movement of the control house within that radius to any desirable position for best observance of the propeller.

The acquisition of data is accomplished manually in that gages and meters are read by an observer and the values written down on suitable forms. There is however, a capability of automated data acquisition with the addition of a considerable amount of auxilliary equipment. Essentially there are two sets of gages on the control console panel. Each set contains a tachometer, a thrust meter, and a torque meter. The operator's thrust and torque meter are calibrated to read percent of allowable thrust and torque while the observer's meters are calibrated to read pounds of thrust and inch-pounds of torque. Both of the tachometers read the propeller rpm. At the outset it was considered that panel meters should be adequate for the acquisition of the data from the test rig but after the dynamometer was operational and some experience had been gained with the generation of performance data it became apparent that the fluctuations of readings did not permit great enough accuracy in the determination of thrust and torque. Consequently, a digital voltmeter was procured for the purpose of reading the millivolt signals from the strain gage balances for both thrust and torque. In some cases where the thrust or torque is extermely low it is advantageous to condition the output of the strain gage bridge by putting it through a DC amplifier then reading the amplified output with the digital voltmeter. With this system small changes in thrust and torque are readily observed. Operational experience has indicated that fine accuracy is very difficult to

achieve when operating at low power coefficients. Apparently the accumulation of gear train and coupling backlash together with the normal torque impulses of the engines contribute to unsteady torque at the propeller. As Cp reaches .025 to .03 the torque indications smooth perceptably and then become quite stable from Cp=.07 on to the maximum for the test. At Cp=.07 and above, the smoothness and repeatability of both the thrust and torque measuring channels is quite good and appears to be repeatable within 2% for repetitive tests.

The slipring assembly originally used for transmission of the propeller balance strain gage signals caused considerable trouble in the initial stages of operation. Brush wear seemed excessive and because of inadequate air blast scavenging, the displaced brush particles were deposited around the inner walls of the brush holding assembly. These deposits provided variable resistance circuits between adjacent brushes and resulted in large fluctuations and zero shifts in the strain gage bridge out put circuits. Cleaning of the slipring assembly was required after about 5 hours of operation and because of the necessity to recalibrate the data acquisition system after each disassembly the down-time was at least three days.

A slipring assembly having adequate cooling and scavenging provisions was installed during the month of July 1965 and has operated satisfactorily and without attention since that time. Some zero-shift between the beginning and end of each test run continues to be manifested, especially during the first 10-15 minutes of operation while the slipring assembly is cold. It has been observed that if the dynamoneter is run for 20 or 30 minutes prior to taking any data, the zero-shift is reduced to insignificant values. With careful calibration and adjustment of the

bridge power supplies, it appears possible to generate data which is repeatable within 2% of the measured performance of the propeller for Cp greater than .025.

A typical performance test for 5 foot diameter propellers requires the determination of thrust and torque for a range of rotational speeds from an arbitrary low value of 1500 RPM to the maximum allowable for the propeller being tested in approximately 200 RPM increments. The blade is set at a predetermined blade angle for each test run, the usual practice is to vary the blade angle at the reference station from zero to 25 degrees in 2.5 degree increments. Various performance parameters are calculated on the University's 7094 computer from the basic values of thrust, torque and rotational speed for each condition and blade angle tested.

Typical performance charts developed from reduced data are presented in another section of this report. Two basic propellers are represented; Propeller A was designed and manufactured several years ago for use with a tilt-wing VTOL model tested in the Langley 30 ft.-by 60 ft-low speed wind tunnel. Propeller B is a model of a propeller currently in use on a tilt-wing VTOL aircraft. (See Figures 1 and 2). Figures 3, 4, and 5 present the performance of these two propellers from experimental data provided by the Texas A&M University static thrust dynamometer. The data points shown in Figures 3,4 and 5 are taken from basic plots of Ct vs Vt, Cp vs Vt and FM vs Vt for each blade angle tested. The plotted points on the basic plots are connected by point-to-point fairing and the values for the composite plots are then read off and plotted for the desired tip speed.

In order to provide visual evaluation of the airflow surrounding the propeller, a smoke generator with appropriate nozzles has been

developed. In addition to the smoke generator, a slavestrobe unit was purchased which permits a gas discharge flashtube to be synchronized at any desired propeller speed. The usual flow visualization technique required the light to flash once per revolution of the propeller. With the smoke generator discharging a filament of smoke at a prescribed point while being illuminated by the flashes of the slavestrobe, an observer is able to get an idea of the relative airflow velocity at various points as well as the direction of airflow through the propeller. In addition to visual observation of the airflow phenomenon, photographs with 3,000 ASA Polaroid film have been made. These photographs show the general inflow pattern of air into the propeller as well as the vortex system that is formed in the wake of the propeller. The helical path of the airflow in the propeller slip stream also is observable thus the introduction of smoke at various points around the rotating propeller has provided a three-dimensional evaluation of the flow phenomenon associated with the propeller operating in the highly loaded static thrust condition. The flow visualization technique by use of smoke filaments will also be useful in determining desirable locations for various airflow velocity and direction measuring equipment to be used during the second year of this project. The strobe light photographic technique is patterned after a similar one observed in operation at Canadair LTD. Montreal, Canada.

Figures 6, 7, 8 and 9 contain photographs of some of the flow visualization experiments made during the development of the smoke filament visualization technique. Of major interest is the magnitude of radial inflow upstream of the propeller and the tip vortex system that is usually seen at approximately .85 R.

All of the work performed during this first year of operation has been essentially of a developmental nature wherein two different

propeller designs having two, three and four blades were extensively tested to determine the reliability and repeatability of the dynamometer. All of the smoke pictures taken to date have been for the purpose of developing the flow visualization technique with very little emphasis being placed upon the use of the data in the analytical effort. Work is currently in progress to further refine the flow visualization technique in an attempt to obtain information which will be useful in the evaluation of the analytical methods under consideration.

THEORY

For many years the theory developed by Goldstein [1] has provided a reliable means of calculating propeller performance. Modified by experience factors and empirical corrections, this theory has been used intensively in the design of propellers, largely for climb and cruise conditions of operations. Attempts to optimize propeller designs for static thrust operation have indicated discrepancies between theoretical performance and actual performance achieved when the Goldstein theory is applied. This research is directed toward investigating these discrepancies and attempting to develop improved methods of calculating propeller performance for the static thrust condition.

Some of the possible discrepancies between the mathematical model postulated in the Goldstein theory and the physical flow situation are apparent.

1. Some of the power put into the propeller is lost in generating the trailing vortex field of the propeller wake. The theory assumes, following Betz [2], that the load distribution on the propeller blade is such as to minimize this power loss for a given thrust. In the heavily loaded static thrust condition

---

Superscript numbers refer to references listed.

there is no assurance that such an optimum load distribution is achieved.

2. As stated by Goldstein, the theory is valid only for small values of the ratio of the displacement velocity of the assumed helical vortex sheet to the velocity of advance of the propeller. Since this ratio becomes infinite in the static thrust condition it sppears to be overly optimistic to expect the theory to hold with good accuracy in this situation.
3. The assumption of the propeller wake being in the form of helical vortex sheets of uniform pitch will be violated in the region immediately downstream of the propeller. In this region, herein called the near wake, the flow is accelerating in the axial direction and hence, the pitch is increasing. The near wake will be dominant in determining the inflow velocity field associated with the trailing vorticity. In addition, the instability of the vortex sheet and the tendency to roll up into discrete vortices will affect the inflow.

If the inflow field can be determined accurately it should be possible to calculate the overall performance of a propeller using two-dimensional airfoil data and a conventional strip-analysis method. The interdependence of the blade load distribution, the trailing vortex field and the inflow velocity field poses a difficult problem that may not be amenable to a direct analytic solution. However, numerical solutions may be devised which with presently available high speed computers will provide useful methods of design optimization. With this in mind, the literature in this field has been surveyed. Publications not referred to explicitly in the list of references are listed in the bibliography appended to this report.

Two methods of calculating the inflow velocity fields have been selected for use in this investigation. They are the method of Iwasaki [3] which is an extension of methods presented by Kucheman [4] and the method of Wu[5]. Both methods involve an initial knowledge of the blade loading and so lend themselves to iterative procedures. In the experimental part of this program, inflow velocity fields will be measured for comparison with those obtained from theory. The calculations by the method of Iwasaki have not been carried out but are planned for a later stage of this program. A procedure for calculations following the theory of Wu has been programmed and is presently in use. This will be discussed below.

In the approach used by Wu the propeller is regarded as an actuator disk, normal to a uniform, steady flow of an incompressible, inviscid fluid. Referred to a cylindrical coordinate system (r,θ, Z) with the Z axis coincident with the axis of rotation, positive direction downstream, the fluid velocity components are (u,v,w,) respectively in the radial, tangential and axial directions. Since the flow is steady and axisymmetric a stream function Ψ can be expressed as a function of r and z from which two of the fluid velocity components u and w can be determined as

$$u = -\frac{1}{r}\frac{\partial \Psi}{\partial z} , \qquad w = \frac{1}{r}\frac{\partial \Psi}{\partial r} . \tag{1}$$

The tangential velocity component v, must be specified separately. Considerations of conservation of angular momentum of the fluid show that the product vr must be a function of Ψ in the slipstream and zero elsewhere.

Writing the equations of motion of the fluid in terms of the stream function results in

$$vr = f(\Psi) \quad \text{in the slipstream}$$
$$= 0 \text{ elsewhere} \tag{2}$$

$$\frac{\partial^2\Psi}{\partial r^2} - \frac{1}{r}\frac{\partial\Psi}{\partial r} + \frac{\partial^2\Psi}{\partial z^2} = (\Omega r^2 - vr)\frac{d(vr)}{d\Psi} \qquad (3)$$

where Ω is the constant angular velocity of the propeller.

This constitutes a set of non-linear, partial differential equations for Ψ and v. Two difficulties arise in obtaining solutions to these equations; namely, the nonlinearity apparent in the terms of the right-hand side of (3) and the fact that the slipstream region is not known.

These equations can be written in dimensionless form normalizing on the radius R as the unit of length and the remote uniform velocity, W. Utilizing differential operators that apply in a linear fashion and a perturbation stream function, ψ , it is possible to express the stream function Ψ , in a non-linear, integral equation with the domain of integration not defined.

Since the domain of integration is determinable from the stream function a method of successive approximations is suggested. The problem of existence and uniqueness of solutions so obtained is mentioned by Wu but not treated by him. In addition, in the numerical calculation procedures some problems of numeric instabilities and lack of convergence in the iterative procedures have appeared.

Only the relations pertinent to the calculation procedure will be presented here. For the complete development the reader is referred to Wu's report.

The approach used in this study is to retain the equations developed in dimensionless form, normalizing on W, the remote velocity. Attempts will be made to extrapolate to the static thrust condition of W=0. This is done to facilitate the numerical calculation procedure which

involves an initial assumption of a stream function corresponding to the free stream flow undisturbed by the actuator disk. For the static thrust condition this would reduce to the trivial case of $W = 0$ at all points or Ψ = constant, which will not provide the required starting point for the calculation. If it becomes necessary to use equations normalized on some other velocity such as tip speed, $R\Omega$, modifications may be made to the calculation procedures.

CALCULATION PROCEDURE

A program for calculation of the inflow velocity field following the method of Wu has been written in the Fortran IV language utilizing the double precision feature of this language. The calculations are carried out on the IBM 7094 located at the Data Processing Center of Texas A&M University. The assistance of J. C. Forehand and J. Vallhonrat of the Data Processing Center staff is gratefully acknowledged.

To provide flexibility and facilitate changes in the program that may be necessary, the program is written in modular form. A flow chart of the main program, identifying the major subroutines, is shown in Figure 10. The numbers shown adjacent to the subroutine titles are the equation numbers as given in Wu's report. These same equation numbers are used in the discussion that follows. The equations are summarized in Appendix I.

LOGIC OF THE MAIN PROGRAM

A parameter card is read with the number of stations on the blade, the maximum tangential component of the fluid velocity, advance ratio, and the number of iterations required.

The initial estimates of $\Psi_o(r)$ are computed as indicated by equation (20). At this point the a_n are computed by equation (32) from

the r, v and Ψ_o (r). Then the b_n are calculated from equation (35b) as they are only dependent on advance ratio and the a_n.

Now the first correction to Ψ (r) is made by calculating ψ (r) as per equation (37) which depends on the b_n and r's exclusively.

As the process is in a developmental stage it is convenient to print out all the intermediate values, therefore the a_n, b_n and ψ (r) are printed at this point. These steps described above are the initializing steps for the iterative process that follows.

The axial component of the fluid velocity, w, is computed from equation (38) then the radial component, u, is calculated for the tip of the blade only by equation (39).

The asymptotic dimensions A_1 and B_1 are given by equations (42) which are only dependent on the b_n.

At this point the first iteration is finished and quantities such as γ, μ and ν are computed from equations (44), (49) and (50) in preparation for the second iteration. The results from the first iteration are now printed.

The calculation of the c_n by equation (46) corresponds to the calculation of the a_n. The c_n depend on the Ψ (r), the r's and v. The k_n are calculated by equation (51b), which correspond to the b_n of our initialization. The σ_n are given by equation (51c).

Next compute ψ(r), the correction to Ψ (r), as per equation (54a), and replace the old b_n with the newly computed k_n and iterate again starting with the computation of the axial fluid velocity component (w) from equation (38).

The iterative process is halted when the number of iterations requested is achieved instead of being based on some convergence

criteria. This was done mainly to permit an evaluation of the convergence characteristics.

At this point a new parameter card is read and the entire process started again.

The main program contains the entire logic of how to go about the solution of the problem with a series of subroutines performing the calculations described in the paper by Wu. Most of the subroutines are perfectly well described by the corresponding formulas, others will need some extra explanation.

The subroutine AGEN for equation (32) computes the a_n by matrix inversion in place using Gaussian elimination. If the number of stations on the blade is large and the stations equally spaced on the blade, the coefficients of a_n will cover a large range of values and therefore, due to the limited precision allowable on the computer, the matrix of coefficients will be singular. In order to have more stations on the blade and avoid singularity of the coefficient matrix it is necessary to concentrate the stations towards the tip of the blade.

The subroutine UGEN for equation (39) at the present time evaluates the integral by successive summation of rectangles and by using a table of complete elliptic integrals built into the program.

The subroutine PSIGN2 for equation (54a) is the most complex one in the entire system. The evaluation of $\hat{\psi}(r)$ according to equation (52) is straight-forward. To calculate the correction terms one first calls subrouting LEGNDP which evaluates integrals of the form $\int_a^b f(x)dx$ by Gaussian quadrature using the zeros and Christoffel numbers of the Legendre polynomials orthogonal over the range -1 to +1. The subroutine LEGNDP needs a function subprogram H2INT to evaluate f(x) which in the

case of the first correction term is

$$f(x) = H_2(\rho)\, d\rho \int_0^{\infty} \frac{J_1(rt)\, J_1(\rho t)}{t + \gamma_1}\, dt$$

But H2INT has to evaluate the above integral. It will evaluate $H_2(\rho)$ as per equation (54b) and LAGRDP which evaluates integrals of the form $\int_a^{\infty} g(x)\, dx$ by Gaussian quadrature using the zeros, and non-weighted and weighted Christoffel numbers of the Laguerre polynomials orthogonal over the range zero to infinity. The subroutine LAGRDP needs in turn a function subprogram (BESI) to evaluate $g(x)$ which in this case is

$$g(x) = \frac{J_1(rt)\, J_1(\rho t)}{t + \gamma_1}$$

Now two Bessel functions of the first kind and first order have to be evaluated so subroutine BESSEL is called. This subroutine computes values of the Bessel functions of the first and second kinds, $J_n(x)$ and $Y_n(x)$, and of the modified Bessel functions of the first and second kinds, $I_n(x)$ and $K_n(x)$ of integral orders n for any value of the argument x. Power series expansions are used for $x \leq n + 6$ and asymptotic expansions for $x > n + 6$.

This process has to be repeated for both the second and third correction terms also. In the first attempt to evaluate equation (54a), only $\hat{\psi}_2(r)$ was evaluated as the author indicates that the contribution of the correction terms is rather small compared to $\hat{\psi}_2(r)$. When the correction terms were added to the process the overall running time increased by a factor of approximately forty.

An upper limit of ten iterations has been used in the calculation procedure in its present stage of development. As mentioned earlier, this approach provides an opportunity to examine the convergence characteristics of the method. Wu states that the second iteration

provides results that are in general sufficiently accurate. At present we cannot agree with this. We find an instability developing in the third iteration that casts doubt on the accuracy of the second iteration. Changes in the iteration procedure are presently being made to eliminate this numeric instability.

CONCLUSIONS

A static-thrust dynamometer has been constructed and calibrated which yields performance data on model propellers with good repeatability. Model blades providing single parameter variation of blade plan-form and twist distribution have been designed. Data from these tests should provide some insight into the effects of these physical parameters on overall static thrust performance.

Flow visualization techniques have been developed that will provide additional information as to the inflow velocity field and the near wake of highly loaded propellers.

A computer program providing a means of calculating the inflow velocity field at the plane of the propeller and the wake contraction has been developed. This program will provide data for comparison with another theoretical program to be developed and with experimental data to be generated later.

REFERENCES

1. Goldstein, S.: On The Vortex Theory of Screw Propellers. Proc. Royal Society, A 123, 1929.

2. Betz, A.: Gottinger Machr., pp. 193-213, 1919.

3. Iwasaki, M. : Diagrams For Use In Calculation of Induced Velocity by Propellers. Kyushu University, Reports of Research Institute for Applied Mechanics, Vol. VI, No. 23, 1958.

4. Kucheman, D. and Weber, J.: Aerodynamics of Propulsion. McGraw-Hill, 1953.

5. Wu, T. Y.: Flow Through a Heavily Loaded Actuator Disk. Schiffstechnik, Band 9, Heft 47, 1962.

BIBLIOGRAPHY

1. Anthony, Robert R., "Simulation of Helicopter and V/STOL Aircraft" Volume IV, U. S. Naval Training Device Center, Technical Report NAVTRADEVCEN 1205-4, December, 1964.

2. Brady, W. G. and Crimi, P., "Representation of Propeller Wakes By Systems of Finite Core Vortices", Summary Report ONR Contract No. Nonr 3691(00), CAL Report No. BB-1665-S-2, February, 1965, Cornell Aeronautical Laboratory, Inc.

3. Brady, W. G., "Theoretical and Experimental Studies of Airfoil Characteristics in Nonuniform Sheared Flow", U. S. Army Aviation Materiel Laboratories, USAAML Technical Report 65-17, May, 1965.

4. Byrd, Paul F. and Friedman, Morris D., "Handbook of Elliptic Integrals for Engineers And Physicists", Springer-Verlag, 1954.

5. Castles, Jr., Walter, Deleeuw, Jacob Henri, "The Normal Component of the Induced Velocity in the Vicinity of a Lifting Rotor and Some Examples of Its Application", NACA Technical Note 2912, March, 1953.

6. Coleman, Robert P., Feingold, A. M., and Stempin, C. W., "Evaluation of the Induced-Velocity Field of An Idealized Helicopter Rotor", NACA War Time Report L-126, June, 1945.

7. Corson, Jr., B. W., and Maynard, Julian D., "The Langley 2,000-Horsepower Propeller Dynameter and Tests at High Speed of an NACA 10-(3X08)-03 Two-Blade Propeller", NACA Technical Note 2859, December, 1952.

8. Crigler, John L. and Jaquis, Robert E., "Propeller-Efficiency Charts for Light Airplanes", NACA Technical Note No. 1338, July, 1947.

9. Critzos, Chris C., Heyson, Harry H. and Boswinkle, Robert W., Jr., "Aerodynamic Characteristics of NACA 0012 Airfoil Section at Angles of Attack From 0^{o} to 180^{o}", NACA Technical Note 3361, January, 1955.

10. Davidson, Robert E., "Linearized Potential Theory of Propeller Induction In A Compressible Flow", NACA Technical Note 2983, September 1953.

11. Deland, J. B. and Carmel, M. M., "Tests of Two-Blade Propellers In the Langley 8-Foot High-Speed Tunnel To Determine The Effect On Propeller Performance Of A Modification of Inboard Pitch Distribution", NACA Technical Note 2268, February, 1951.

12. DeYoung, John, "Propeller At High Incidence", Journal of Aircraft, Volume 2, Number 3, May-June, 1965.

13. Durand, W. F. (Editor), "Aerodynamic Theory", Volume IV, Divisions J-M.

14. Erickson, Jr., J. C., Ladden, R. M., Borst, H. V. and Ordway, D. E., "A Theory For VTOL Propeller Operation In A Static Condition", U. S. Army Aviation Materials Laboratories, USAAVLABS Technical Report 65-69, October, 1965.

15. Foss, R. L., "Strip Analysis Method For Evaluating Static Thrust", Curtiss-Wright Corporation, Report C-2402, 1952.

16. Glauert, H., "The Elements of Aerofoil And Airscrew Theory", Cambridge - At The University Press, 1947.

17. Goodson, Kennth W. and Grunwald, Kalman J., "Aerodynamic Characteristics of a Powered Semispan Tilting-Shrouded-Propeller VTOL Model in Hovering and Transition Flight", NASA Technical Note D-981, January, 1962.

18. Greenberg, M. D. and Ordway, D. E., "The Ducted Propeller in Static and Low-Speed Flight", Therm Advanced Research, Inc., TAR-TR 6407, October, 1964.

19. Grunwald, Kalman J. and Goodson, Kennth W., "Aerodynamic Loads On An Isolated Shrouded-Propeller Configuration For Angles Of Attack From -10° To 110°", NASA Technical Note D-995, January, 1962.

20. Hamilton Standard, "Static Thrust Additions To Strip Analysis", Hamilton Standard Division, United Aircraft Corporation.

21. Hough, Gary R. and Ordway, Donald Earl, "The Steady Velocity Field Of A Propeller With Constant Circulation Distribution", Journal Of The American Helicopter Society, Vol. 10, No. 2, April, 1965.

22. Kawada, Sandi, "Induced Velocity By Helical Vortices", Journal of Aeronautical Sciences, Volume 3, 1936.

23. Knight, Montgomery and Hefner, Ralph A., "Analysis of Ground Effect on the Lifting Airscrew", NACA Technical Note No. 835, December, 1941.

24. Knight, Montgomery and Loeser, Oscar Jr., "Pressure Distribution Over A Rectangular Monoplane Wing Model Up To 90° Angle of Attack", NACA Report No. 288, 1928.

25. Knight, Montgomery and Hefner, Ralph A., "Static Thrust Analysis Of The Lifting Airscrew", NACA Technical Note No. 626, December, 1937.

26. Knight, Montgomery and Wenzinger, Carl J., "Wing Tunnel Tests On A Series of Wing Models Through A Large Angle of Attack Range", NACA Report No. 317, 1929.

27. Kriebel, A. R., "Theoretical Investigation of Static Coefficients, Stability Derivatives, and Interference For Ducted Propellers", Vidya Report No. 112, March 31, 1965.

28. Kuhn, Richard E. and Hayes, William C., Jr., "Wind-Tunnel Investigation of Longitudinal Aerodynamic Characteristics of Three Propeller-Driven VTOL Configurations in the Transition Speed Range, Including Effects of Ground Proximity", NASA Technical Note D-55, February, 1960, Eng. Lib.

29. Lerbs, Dr. Hermann W., "An Approximate Theory of Heavily Loaded, Free-Running Propellers in the Optimum Condition", The Society of Naval Architects and Marine Engineers Transactions, Volume 58, 1950.

30. Lerbs, Dr. H. W., "Moderately Loaded Propellers With A Finite Number of Blades And An Arbitrary Distribution of Circulation", The Society of Naval Architects and Marine Engineers Transactions, Volume 60, 1952.

31. Meyer, Jr., John R., "An Investigation of Bending Monment Distribution On A Model Helicopter Rotor Blade And A Comparison With Theory", NACA Technical Note 2626, February, 1952.

32. Meyer, Jr., John R., and Falabella, Jr., G., "An Investigation Of The Experimental Aerodynamic Loading On A Model Helicopter Rotor Blade", NACA Technical Note 2953, May, 1953.

33. Miller, R. H., "Unsteady Airloads on Helicopter Rotor Blades", Presented to The Royal Aeronautical Society, Rotorcraft Section, October 25, 1963.

34. Nikolsky, Alexander A., "Helicopter Analysis", John Wiley & Son, Inc., 1951.

35. Payne, P. R., "Helicopter Dynamics and Aerodynamics", The Macmillian Company, 1959.

36. Reid, Elliott G., "Studies Of Blade Shank Form and Pitch Distribution For Constant-Speed Propellers", NACA Technical Note No. 947, January, 1945.

37. Reid, Elliott G., "Wake Studies of Eight Model Propellers", NACA Technical Note 1040, July, 1946.

38. Rogallo, V. L., Roberts, J. C. and Oldaker, M. R., "Vibratory Stresses In Propellers Operating In The Flow Field Of a Wing-Nacelle-Fuselage Combination", NACA Technical Note 2308, March, 1951.

39. Salters, Leland B. Jr. and Norton, Harry T. Jr., "An Investigation Of The Effect Of The WADC 30,000-Horsepower Whirl Rig Upon The Static Charactistics of A Propeller", NACA Research Memorandum

RM SL52F20, July 1952.

40. Sipe, Jr., O. E. and Gorenberg, N. B., "Effect of Mach Number, Reynolds Number, And Thickness Ratio On The Aerodynamic Characteristics of NACA 63A-Series Airfoil Sections", U. S. Army Aviation Materials Laboratories, USAAML Technical Report 65-28, June, 1965.

41. Slaymaker, S. E. and Gray, Robin B., "Power-Off Flare-Up Tests Of A Model Helicopter Rotor In Vertical Autorotation", NACA Technical Note 2870, January, 1953.

42. Stewart, H. J., "The Aerodynamics Of A Ring Airfoil", Quarterly of Applied Mathematics, Vol. 2, 1944-1945.

43. Tanner, Watson H., "Charts For Estimating Rotary Wing Performance In Hover and At High Forward Speeds", NASA CR-114, November, 1964.

44. Tanner, Watson H., "Tables For Estimating Rotary Wing Performance At High Forward Speeds", NASA CR-115, November, 1964.

45. Tapscott, Robert J. and Kelley, Henry L., "A Flight Study Of The Conversion Maneuver Of A Tilt-Duct VTOL Aircraft", NASA Technical Note D-372, November, 1960.

46. Taylor, Marion K., "A Balsa-Dust Technique For Airflow Visualization And Its Application To Flow Through Model Helicopter Rotors In Static Thrust", NACA Technical Note 2220, November, 1950.

47. Theodorsen, Theodore, "Theory of Propellers", McGraw-Hill Book Company, Inc., 1940.

48. Thomas III, Lovic P., "A Flight Study Of The Conversion Maneuver Of A Tilt-Wing VTOL Aircraft", NASA Technical Note D-153, December, 1959.

49. Von Mises, Richard, "Theory of Flight", McGraw-Hill Book Company, Inc., 1945.

50. Watson, G. N., "Theory of Bessel Functions", Second Edition, Cambridge - At The University Press, 1944.

51. Watts, J. A., "Static Performance Characteristics of 5 Propellers As Measured On The Canadair Propeller Test Stand, With A Flow Visualization Survey of One Propeller", Report - RAX-84-112, Canadair Limited, 1963.

52. Watts, J. A., "Analysis of the Effects of Activity Factor, Loading, Twist, Scale and Mach Number on the Static Performance of Propellers", Addendum To Report RAX-84-112, Canadair Limited, 1964.

53. Yaggy, Paul F. and Mort, Kenneth W., "A Wind Tunnel Investigation Of A 4-Foot-Diameter Ducted Fan Mounted On The Tip of a Semispan Wing", NASA Technical Note D-776, March, 1961.

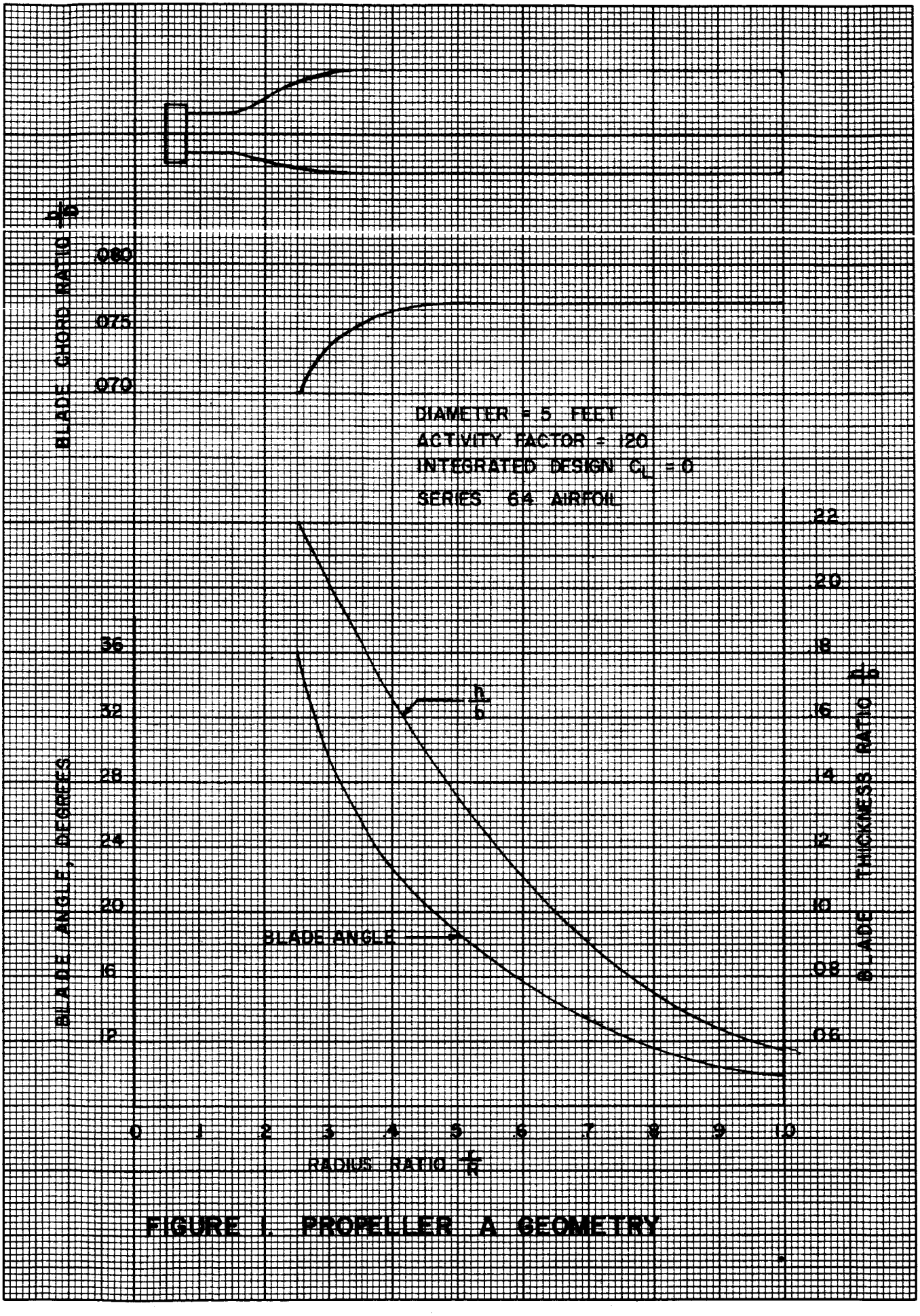

FIGURE I. PROPELLER A GEOMETRY

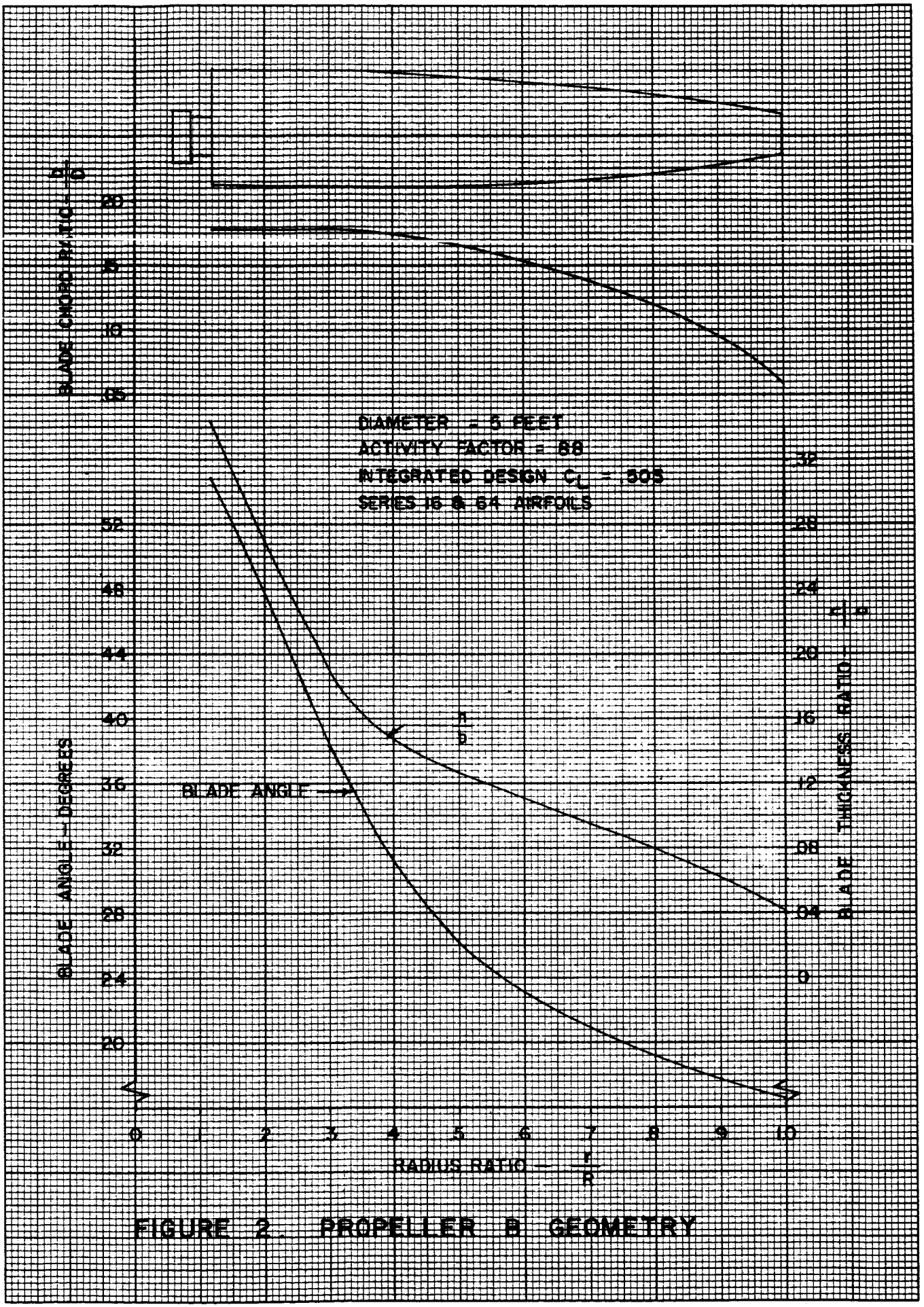

FIGURE 2. PROPELLER B GEOMETRY

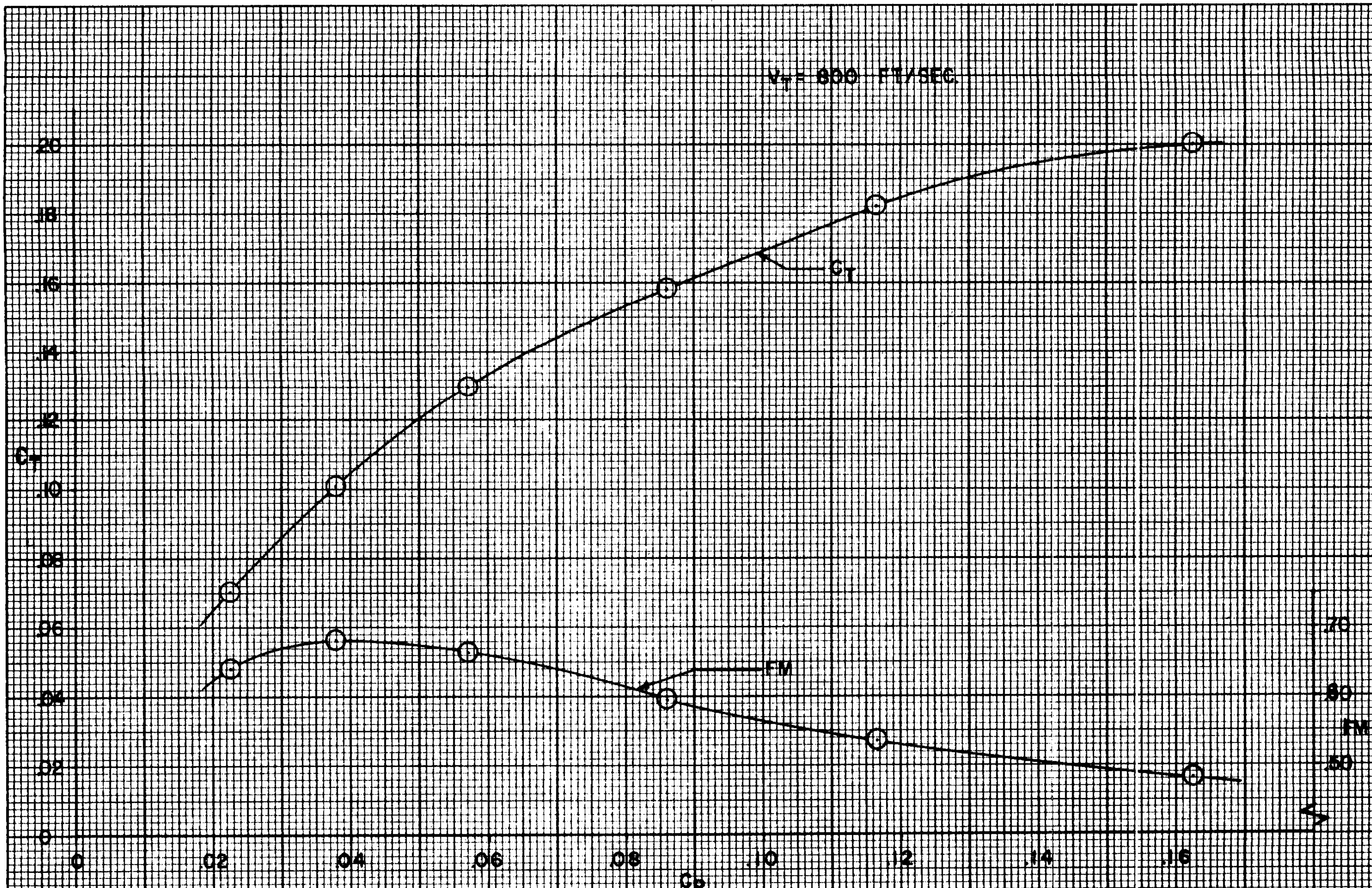

FIGURE 3. C_T AND FM vs C_P FOR 4-WAY PROPELLER A

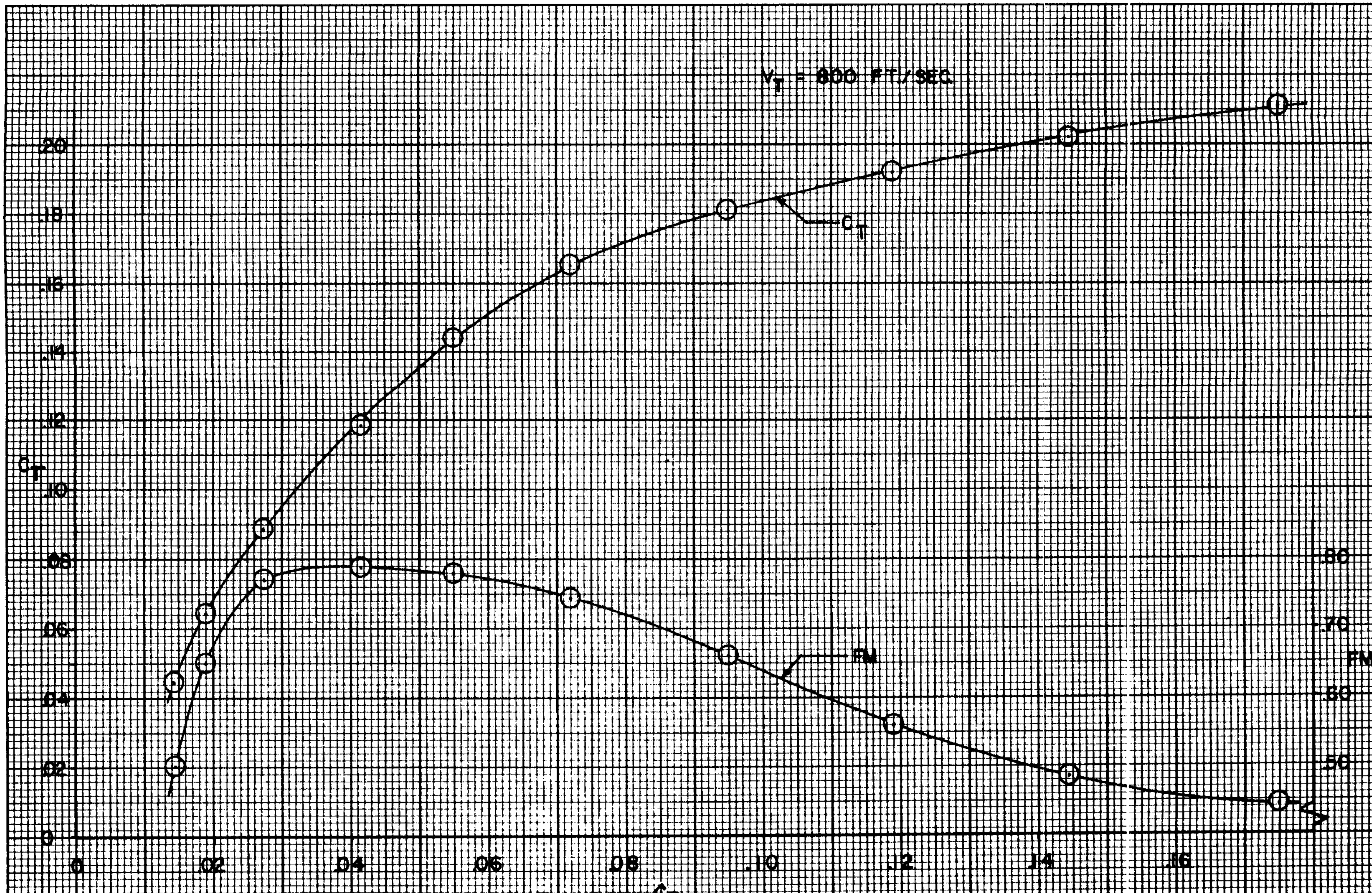

FIGURE 4. C_T AND FM vs C_P FOR 4-WAY PROPELLER B

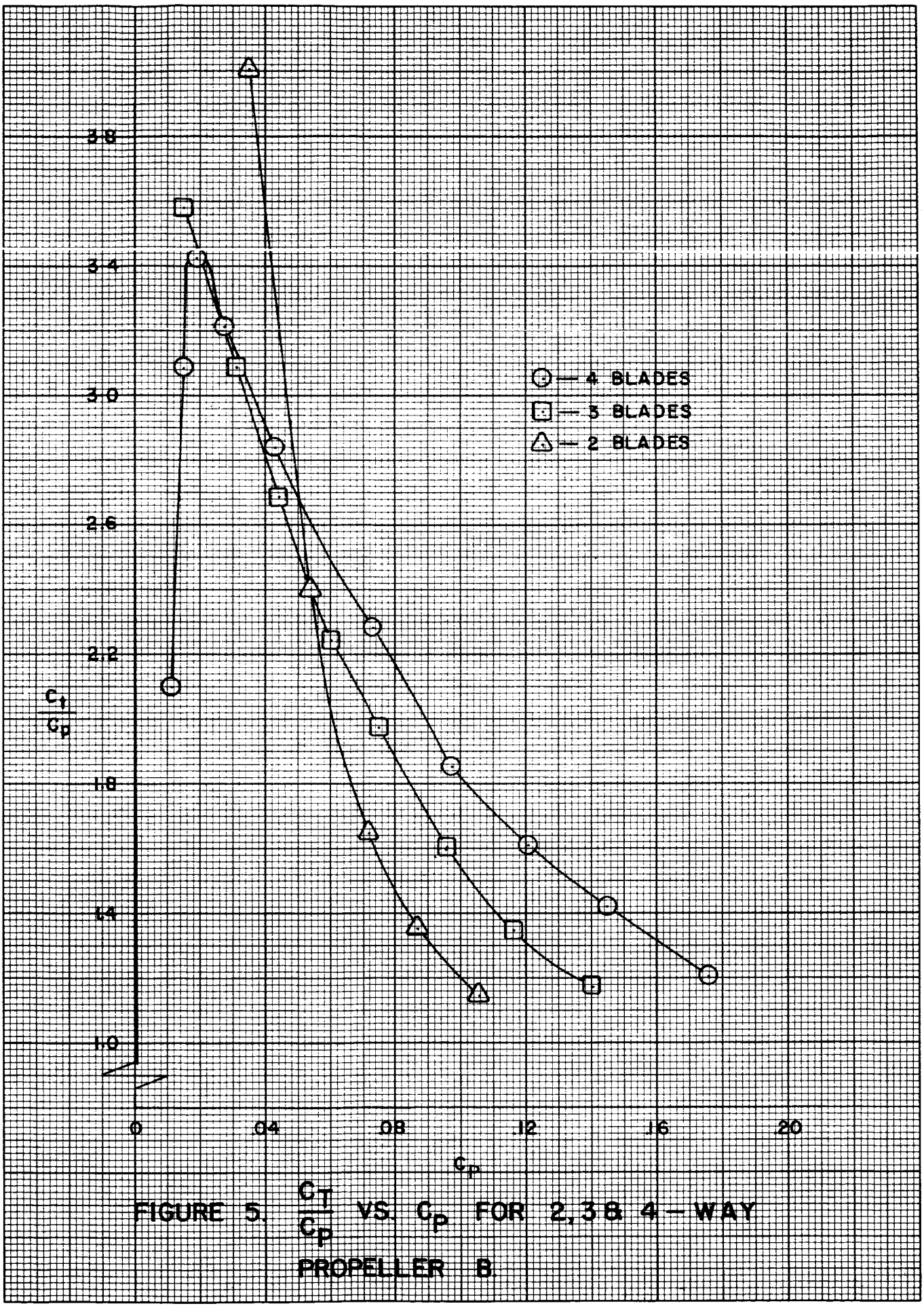

FIGURE 5. $\frac{C_T}{C_P}$ VS. C_P FOR 2, 3 & 4 — WAY PROPELLER B.

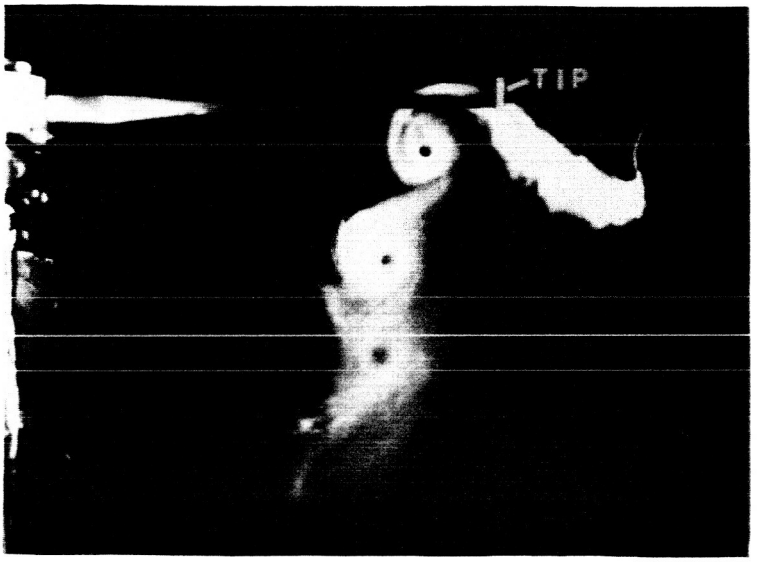

Figure 6. Flow visualization photograph of the tip vortex. The probe is positioned 6 inches outboard and 6 inches downstream of the propeller blade tip.

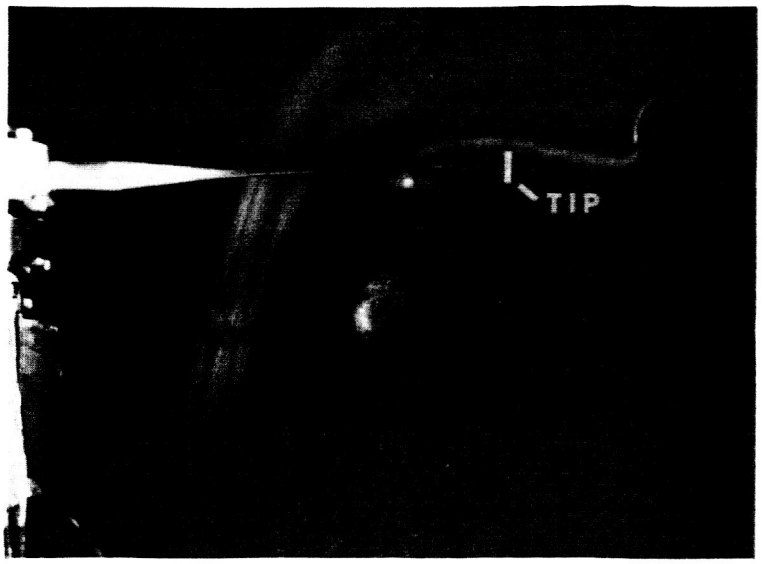

Figure 7. A tip vortex photograph with the probe positioned 6 inches outboard of the propeller tip. Note the smoke sheet with a discontinuity apparently caused by the trailing vortex sheet of the preceding blade.

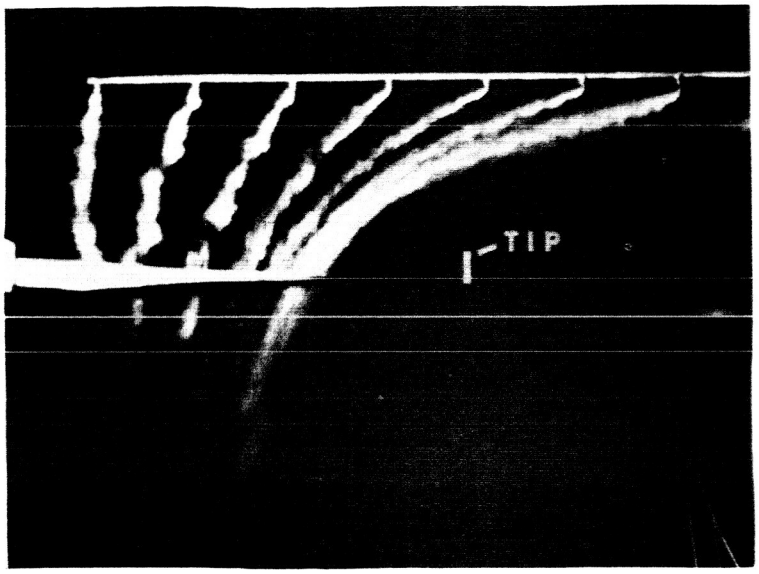

Figure 8. The multi-filament rake is positioned 12 inches upstream of the propeller with the nozzle at the left placed 6 inches outboard of the propeller rotational axis.

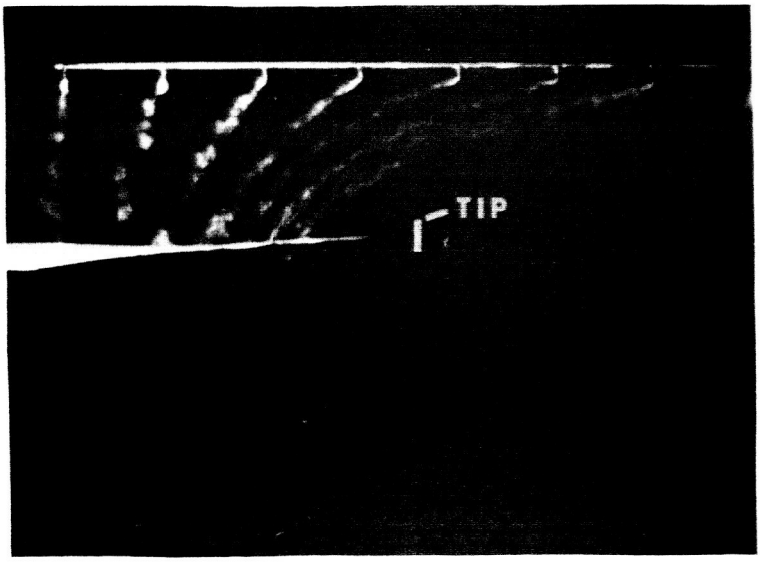

Figure 9. A photograph of the inflow showing the strong radially inward flow approximately 24 inches outboard of the tip.

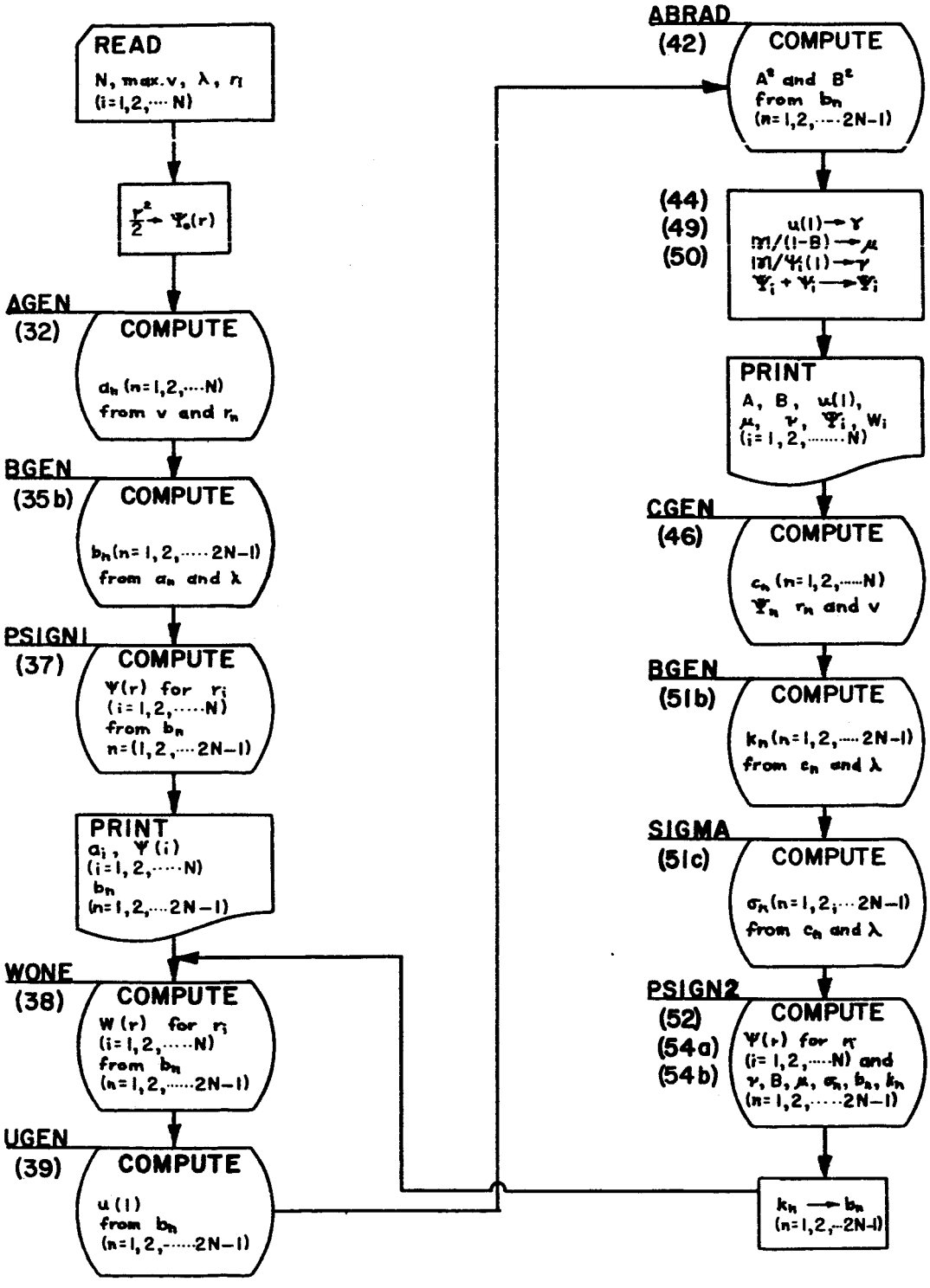

FIGURE 10 MAIN PROGRAM FLOW CHART

APPENDIX I

Equations Used in Numerical Calculations

(The equation numbers are those of Reference 5)

(20) $\Psi(r,z) = \Psi_o(r) + \psi(r,z), \qquad \Psi_o(r) = \frac{1}{2} r^2$

(32) $rv(r,0+) = \sum_{n=1}^{N} a_n (r^2/2)^n, \qquad 0 \le r \le 1$

(35b) $b_n = 2^{-n} \sum_{m=n-N+1}^{N} m a_m a_{n-m+1}, \qquad n = N+1, \cdots 2N-1$

(37) $\psi_1(r,0) = r^2 \sum_{n=1}^{2N-1} \frac{b_n}{8n} \left[1 - \frac{r^{2n}}{n+1} \right]$ for $r \le 1$

(38) $w_1(r,0) = \frac{1}{r} \frac{\partial}{\partial r} (\Psi_o + \psi_1)_{z=0}$

$= 1 + \sum_{n=1}^{2N-1} \frac{b_n}{4n} (1 - r^{2n})$ for $r \le 1$

(39) $u_1(1,0) = - \sum_{n=1}^{2N-1} \frac{b_n}{\pi} \int_0^1 \left[K(\rho) - E(\rho) \right] \rho^{2n-1} d\rho$

(42) $A_1^2 = 1 + \sum_{n=1}^{2N-1} \frac{b_n}{4(n+1)}$,

$B_1^2 = A_1^2 - B_1^2 \sum_{n=1}^{2N-1} \frac{b_n}{2n} \left[1 - \frac{B_1^{2n}}{n+1} \right]$

(44) $\gamma_1 = u_1(1,0)$

(46) $\sum_{n=1}^{N_1} c_n \Psi_1^n(r,0) = \sum_{n=1}^{N} a_n (r^2/2)^n$

(49) $h_1^*(z) = B_1 + (1 - B_1) e^{-\mu_1 z}, \qquad \mu_1 = |\gamma_1| / (1 - B_1),$ for $z \ge 0$.

(50) $\psi_1^*(r,z) = \psi_1(r,0) \left[2 - e^{-\nu_1 z} \right], \qquad \nu_1 = |\gamma_1| / \psi_1(1,0),$ for $z \ge 0$

(51b) $k_n = 2^{-n} \sum_{m=n-N_1+1}^{N_1} m c_m c_{n-m+1}, \qquad n = N_1 + 1, \cdots 2N_1 - 1$

(51c) $\sigma_n = \frac{n}{2^{(n-1)}} \sum_{m=n-N_1+1}^{N_1} m c_m c_{n-m+1} \qquad n = N_1 + 1, \cdots 2N_1 - 1$

$$(52)\quad \psi_2(r,\infty) = r^2 \sum_{n=1}^{2N_1-1} \left[B_1^{2n} - \frac{r^{2n}}{n+1}\right]\left[\frac{k_n}{4n} + \frac{\sigma_n}{16n} \sum_{m=1}^{2N-1} \frac{b_m}{m}\right]$$

$$- r^2 \sum_{n=1}^{2N_1-1} \sum_{m=1}^{2N-1} \frac{\sigma_n b_m}{16m} \frac{B_1^{2(n+m)} - \dfrac{r^{2(n+m)}}{n+m+1}}{(m+1)(n+m)} \quad \text{for } r \le B_1$$

$$(54a)\quad \psi_2(r,0) = \psi_2(r) - \frac{r}{2}\int_0^1 H_2(\rho)\,d\rho \int_0^\infty \frac{J_1(rt)J_1(\rho t)}{t+\nu_1}\,dt$$

$$- \frac{r}{2}\int_{B_1}^1 H_1(\rho)\,d\rho \int_0^\infty \frac{J_1(rt)J_1(\rho t)}{t}\left[\frac{\rho - B_1}{1-B_1}\right]^{t/\mu_1} dt$$

$$+ \frac{r}{2}\int_{B_1}^1 H_2(\rho)\,d\rho \int_0^\infty \frac{J_1(rt)J_1(\rho t)}{t+\nu_1}\left[\frac{\rho - B_1}{1-B_1}\right]^{(t+\nu_1)/\mu_1} dt$$

$$(54b)\quad H_1(r) = \sum_{n=1}^{2N_1-1} k_n r^{2n} + 2H_2(r)$$

$$H_2(r) = \sum_{n=1}^{2N_1-1} \sum_{m=1}^{2N-1} \frac{\sigma_n b_m}{8m}\left[1 - \frac{r^{2m}}{m+1}\right] r^{2n}$$